The American Journal of Human Genetics, Volume *109*

Supplemental information

ADGRL1 haploinsufficiency causes a variable spectrum of neurodevelopmental disorders in humans and alters synaptic activity and behavior in a mouse model

Antonio Vitobello, Benoit Mazel, Vera G. Lelianova, Alice Zangrandi, Evelina Petitto, Jason Suckling, Vincenzo Salpietro, Robert Meyer, Miriam Elbracht, Ingo Kurth, Thomas Eggermann, Ouafa Benlaouer, Gurprit Lall, Alexander G. Tonevitsky, Daryl A. Scott, Katie M. Chan, Jill A. Rosenfeld, Sophie Nambot, Hana Safraou, Ange-Line Bruel, Anne-Sophie Denommé-Pichon, Frédéric Tran Mau-Them, Christophe Philippe, Yannis Duffourd, Hui Guo, Andrea K. Petersen, Leslie Granger, Amy Crunk, Allan Bayat, Pasquale Striano, Federico Zara, Marcello Scala, Quentin Thomas, Andrée Delahaye, Jean-Madeleine de Sainte Agathe, Julien Buratti, Serguei V. Kozlov, Laurence Faivre, Christel Thauvin-Robinet, and Yuri Ushkaryov

Supplemental information

Supplemental Results

Genetic background-dependent embryonic lethality of *Adgrl1*$^{-/-}$ mice

The heterozygous (HET) mice obtained from the chimeric founders on the 129/SvJ genetic background were backcrossed to a more robust C57BL/6 background. Subsequent interbreeding of the 129/SvJ-C57BL/6 mixed-background HET mice produced more than 100 WT and HET progeny, before the first KO pup was identified (Figure S2B-D). Using this animal, the backcrossing to C57BL/6 mice continued for eight additional generations. As a result, a permissive haplotype was achieved, on which many KO animals were born. However, after 324 matings, which produced 234 litters comprising more than 1270 mice born, the established colony still demonstrated sub-Mendelian distribution of the *Adgrl1* allele (Figure S2E), with a clear bias against producing homozygous *Adgrl1*$^{-/-}$ offspring. Specifically, intercrossing two HET mice, on average, produced 1.9 times more WT than KO pups (Figure S2E, left). Likewise, when HET and KO animals were crossed, HET offspring were produced 2.4-fold more frequently than KO offspring (Figure S2E, right). Mating two *Adgrl1* nullizygous mice was also attempted, but out of 5 pairs only one was successful, producing two litters with 2-3 pups in each and killing them each time. HET animals (carrying one WT and one KO *Adgrl1*$^{-}$ allele) survived the gestation well, which indicated that the C57BL/6 genotype was at least partially compensatory, and that the disruptive mutant phenotype was recessive.

The observed paucity of KO progeny could be caused by several problems associated with the disruption of *Adgrl1*, such as low fertility of KO spermatozoa or developmental deficits in KO embryos. Therefore, we examined the relationship between parental genotypes and litter sizes and found that, on average, KO sires produced litters 20% smaller than those of WT sires, while KO dams produced litters 38% smaller than those of WT dams and 30% smaller than those of KO sires (Figure S2F). When considering the survival rate of *Adgrl1*$^{-/-}$ progeny in HET-KO pairs, we found that KO pups were born twice more frequently when the female was HET than if she was KO (Figure S2G). These results ruled

out potential physiological or behavioral abnormalities of the *Adgrl1*-deficient males as the main reason for the underproduction of KO progeny and argued for litter size being dependent on the parents' genotypes, most likely as a consequence of abnormal embryonic lethality of KO conceptuses, especially when carried by KO dams. Indeed, dissection of several pregnant females, at gestation day 16, revealed embryo resorption sites indicative of *in utero* lethality at early stages of embryogenesis (not shown). Although the genotype of these dead embryos could not be established, the sub-Mendelian production of KO pups suggests that they were *Adgrl1*$^{-/-}$.

Behavioral abnormalities in *Adgrl1*$^{-/-}$ mice

While the colony was maintained on the mixed, non-compensatory 129/SvJ-C57BL/6 background, the HET pups born often showed neurodevelopmental abnormalities. In particular, more than 15% of HET pups were unable to move in a coordinated manner. The righting reflex was used to assess the level of arousal. At postnatal day four (P4), when this phenotype was most pronounced, the time required to flip from supine to prone position was 8.7 ± 0.7 s for WT pups and 42.5 ± 9.9 s for HET pups, with some affected animals being unable to right themselves at all and often spontaneously rolling over while attempting to crawl in the prone position. Inability to suckle was another consequence of uncoordinated locomotor activity and the main reason of severe malnourishment and underdevelopment of some HET pups (Figure 3A, middle). Two less affected HET animals survived until weaning, but then demonstrated neurological deficits, such as periodic arrests and focal seizures, especially when introduced into a novel environment (e.g. open space) (Figure 3A, right). These neurodevelopmental defects were not displayed by the WT animals (Figure 3B) and, upon outcrossing on a more permissive background, HET animals developed normally and revealed no behavioral or neurological deviations.

On the permissive C57BL/6 background, many KO animals successfully completed their development but demonstrated consistent infanticide. In 25 out of 27 cases, KO dams killed all the pups in the litter (Figure 3C). Live pups were sometimes observed before they were killed, but most offspring were

killed within the first hour after birth. The dead neonates never showed milk spots, indicating that they had not been nursed by their mother. Each dead pup was either badly mauled or partially eaten, indicating that the mother (and sometimes the father) specifically aimed at killing each newborn. This behavior was consistent with a deliberate act of aggression rather than simple abandonment, lack of maternal care, passive cannibalism of the already dead offspring, or an attempt by the mother to protect herself by consuming her pups for nutrition in view of an outside danger (e.g. a predator). The almost immediate attack on the litter suggested an affective dysfunction, while the more delayed infanticide could also be driven by a cognitive impairment. These results suggested that pups' demands of food and comfort were perceived by the mother as an intensely intrusive stressful stimulus. The neonaticide did not depend on the pups' genotypes or number and, on average, occurred after 58% of parturitions, irrespective of the number of previous parturitions (Figure 3D). In other words, while many KO dams killed each litter, others attacked few of their litters, whereas some KO females only killed one out of several litters. This indicates that the stress caused by the presence of the litter could be conditioned by other factors, so that the anxiety did not always overwhelm the dam's sensory endurance, causing her to eliminate (kill) the source of distress only in ~60% of cases.

KO male mice killed their own offspring in 28.6% of cases (Figure 3C) and showed also no adaptation to subsequent litters, killing on average about 15.5% of litters after each parturition (Figure 3D). KO males, similar to KO females, were apparently unable to process intrusive environmental stimuli, but obviously the situation was less stressful for them than for females, leading to a lower prevalence of paternal infanticide. All pairs consisting of both KO parents killed their offspring (Figure 3C, D), and therefore KO-KO breeding pairs were normally avoided. Pairs, consisting of HET and/or WT animals on the *Adgrl1*$^{-/-}$-compensatory background, never killed their offspring (0 out of 35), while among 31 HET-HET inter-crosses, infanticide occurred only once. These results clearly demonstrate that only KO animals poorly tolerated stressful situations, but this phenotype was not sex-specific.

Supplemental figures and legends

A

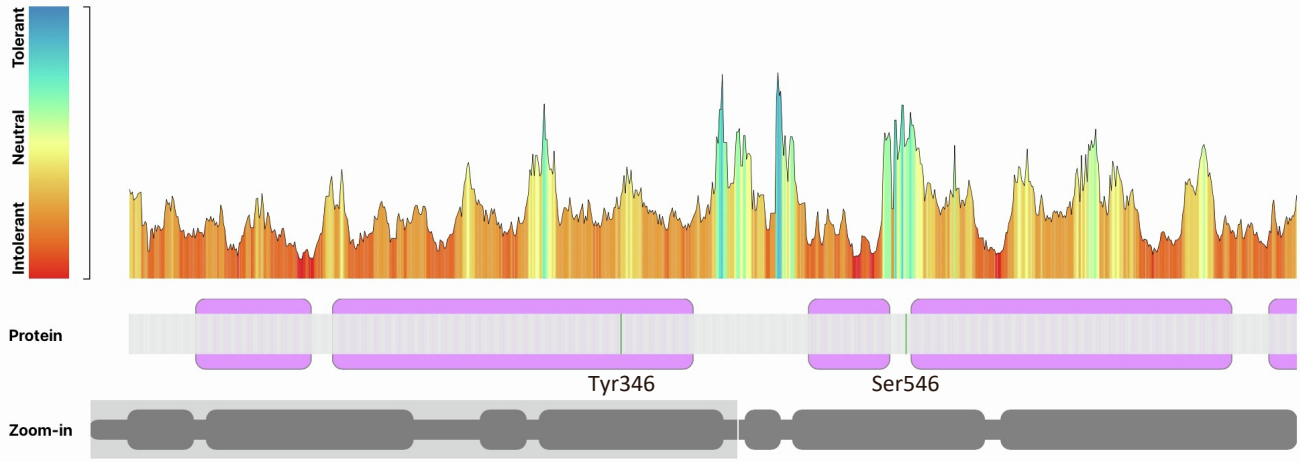
Tolerant
Neutral
Intolerant
Protein
Tyr346
Ser546
Zoom-in

B

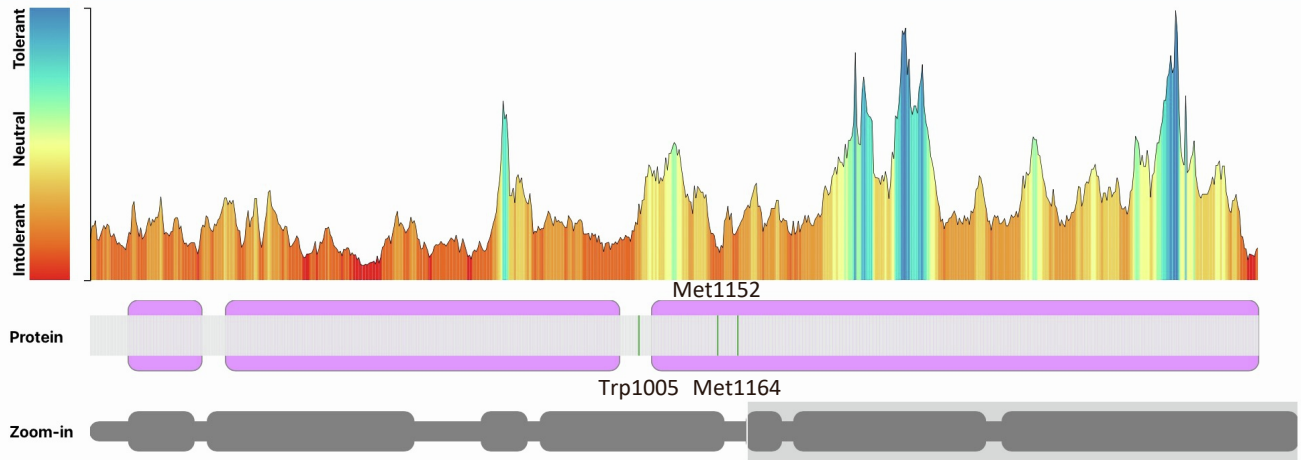
Tolerant
Neutral
Intolerant
Met1152
Protein
Trp1005
Met1164
Zoom-in

Figure S1. Mutation tolerance landscape of ADGRL1 positions discussed in this work. A, Amino acid changes were identified at positions Tyr346 (individual 10 and De Rubeis et al., 2014)[72] and Ser546 (De Rubeis et al.,2014).[72] **B,** Positions Trp1005, Met1152, and Met1164 were affected in individuals 1, 5, and 6 respectively. NM_001008701.2 transcript was used for this analysis.

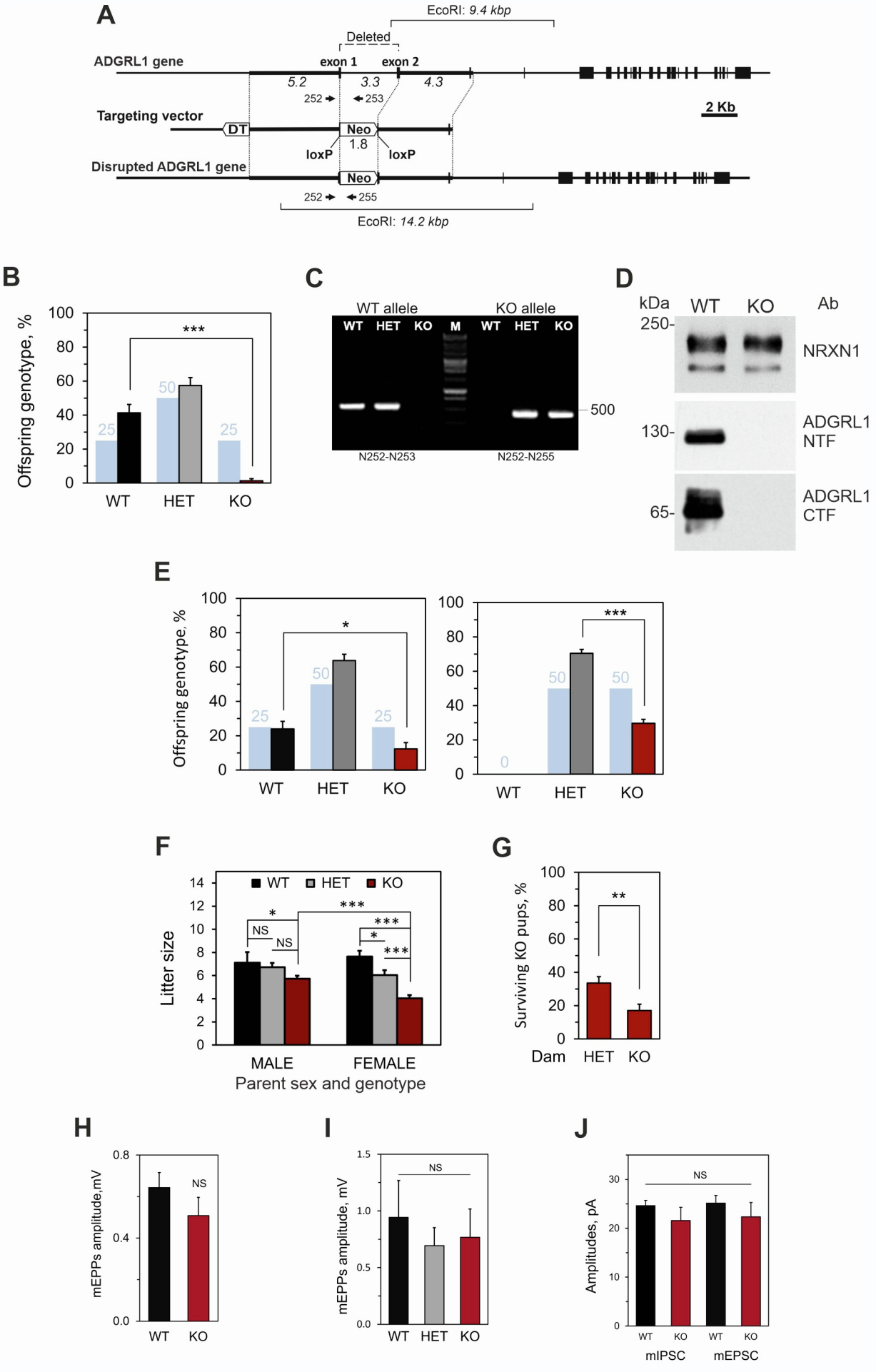
A
EcoRI: 9.4 kbp
Deleted
ADGRL1 gene
exon 1
exon 2
5.2
3.3
4.3
252
253
2 Kb
Targeting vector
DT
Neo
1.8
loxP
loxP
Disrupted ADGRL1 gene
Neo
252
255
EcoRI: 14.2 kbp
B
Offspring genotype, %
100
80
60
40
20
0
***
25
50
25
WT
HET
KO
C
WT allele
KO allele
WT HET KO M WT HET KO
500
N252-N253
N252-N255
D
kDa
WT
KO
Ab
250-
NRXN1
130-
ADGRL1 NTF
65-
ADGRL1 CTF
E
Offspring genotype, %
100
80
60
40
20
0
*
25
50
25
WT
HET
KO
100
80
60
40
20
0
***
0
50
50
WT
HET
KO
F
WT
HET
KO
Litter size
14
12
10
8
6
4
2
0
*
NS
NS
***
***
*
***
MALE
FEMALE
Parent sex and genotype
G
Surviving KO pups, %
100
80
60
40
20
0
**
Dam
HET
KO
H
mEPPs amplitude,mV
0.8
0.4
0.0
NS
WT
KO
I
mEPPs amplitude, mV
1.5
1.0
0.5
0.0
NS
WT
HET
KO
J
Amplitudes, pA
30
20
10
0
NS
WT
KO
WT
KO
mIPSC
mEPSC

Figure S2. Targeted disruption of *Adgrl1*. A, Schematic representation of the targeting event. Top, the original mouse *Adgrl1*. Middle, the targeting vector. Bottom, the resulting inactivated *Adgrl1*. The exons are shown as vertical bars. The brackets above and below indicate Eco RI fragments identified by Southern hybridization of the respective alleles; the numbered arrows represent the primers used for PCR-genotyping. The scale bar is provided on the right. **B**, Sub-Mendelian frequency of the *Adgrl1*$^{-/-}$ neonates in the offspring of HET-HET breeding pairs on a mixed 129/SvJ-C57BL/6 background. Blue bars with values, an expected Mendelian distribution of genotypes, in percent. Bright bars, the real genotypes distribution in offspring (n = 20 litters; 103 pups; $p < 4x10^{-6}$). **C**, Identification of the original and mutant *Adgrl1* alleles using PCR. M, MW markers. **D**, Western blot analysis of ADGRL1 and NRXN1 in WT and KO mouse brains. The image is representative of n = 6 experiments, which gave similar results. **E**, Persistent sub-Mendelian frequency of the *Adgrl1*$^{-/-}$ genotype in the mature colony on the C57BL/6 background. Color coding as in B. Left, genotypes of the progeny of HET-HET breeding pairs (n = 27 litters, 161 offspring; $p < 0.05$). Right, genotypes of the progeny of HET-KO breeding pairs (n = 97 litters, 558 offspring; $p < 3.4x10^{-10}$). **F**, Litter sizes as a function of parental genotypes (litter numbers n = 85 for KO male parent and n = 61 for KO female parent; $p < 1.5x10^{-5}$). In each case, the other parent was WT or HET. **G**, The proportion of KO pups in the offspring of HET-KO pairs, as a function of mother's genotype (HET dams: n = 74 litters, 445 offspring; KO dams: n = 23 litters, 113 offspring; $p < 0.001$). **H**, The amplitudes of spontaneous mEPPs do not differ in WT and KO mice at rest, as in Figure 4C ($p > 0.05$; WT, n = 8; KO, n = 11). **I**, The amplitudes of LTX^{N4C}-evoked mEPPs are similar at the NMJs of WT and HET mice, as in Figure 4G (WT, n = 6; HET, n = 3; KO, n = 5 independent animals). **J**, The amplitudes of mIPSCs and mEPSCs in WT and KO neuronal cultures, as in Figure 4H (n = 28 for each condition).

Supplemental Methods

Exome sequencing and bioinformatics

Several approaches were utilized according to each institution.

Dijon. Libraries of genomic DNA samples were prepared using the Twist Human Core Exome kit (Twist Biosciences, San Francisco, CA), and were sequenced on a NovaSeq 6000 instrument (Illumina, San Diego, CA) according to the manufacturer's recommendations for paired-end 151-bp reads. A mean depth of 86.96 x was reach and 97.2 % of the refseq exons were covered at least by 10 reads.

Variants were identified using a computational platform of the FHU Translad, hosted by the University of Burgundy Computing Cluster (CCuB). Raw data quality was evaluated by FastQC software (v0.11.4). Reads were aligned to the GRCh37/hg19 human genome reference sequence using the Burrows-Wheeler Aligner (v0.7.15). Aligned read data underwent the following steps: (a) duplicate paired-end reads were removed by Picard software (v2.4.1), and (b) base quality score recalibration was done by the Genome Analysis Toolkit (GATK v3.8) Base recalibrator. Using GATK Haplotype Caller, Single Nucleotide Variants with a quality score >30 and an alignment quality score >20 were annotated with SNPEff (v4.3). Rare variants were identified by focusing on nonsynonymous changes present at a frequency less than 1% in the GNOMAD database. Copy Number Variants were detected using xHMM (v1.0) and were annotated using in-house python scripts. They were filtered regarding their frequency in public databases (DGV, ISCA, DDD).

Paris. Sequencing libraries were prepared using the KAPA HyperExome (Roche, Basel, Switzerland) and sequenced as 75-bp paired-end reads on the Nextseq 500 platform (Illumina, San Diego, CA, USA). Reads were processed following a standard analysis pipeline at the Pitié-Salpêtrière University Hospital. Overall sequencing and quality was assessed with FastQC v0.11.8, the reads were then aligned to the reference human genome sequence (hg19) using the Burrows-Wheeler Aligner BWA-mem v0.7.17, the alignment files were sorted and indexed using Samtools v1.9, and Sambamba v0.7.0 was used to flag duplicates. Variants were called using GATK Software v4.1.4. Multi-allelic variants

were split and indels were normalized using vt 0.57721. Variants were annotated with Variant Effect Predictor (v105), and filtered according to population occurrence (gnomAD v2 and v3), impact, and segregation. Copy Number Variants were called using an in-house algorithm. In brief, depth of coverage of a genomic region was compared across the co-sequenced individuals in the same library (n=12). They were analyzed according to population databases (DGV) and co-occurrence in the same run.

GeneDx. Exome sequengin was performed as previously described in Retteret et al.[1] In summary, using genomic DNA from the proband and parents, the exonic regions and flanking splice junctions of the genome were captured using the IDT xGen Exome Research Panel v1.0 (Integrated DNA Technologies, Coralville, IA). Massively parallel (NextGen) sequencing was done on an Illumina system with 100bp or greater paired-end reads. Reads were aligned to human genome build GRCh37/UCSC hg19, and analyzed for sequence variants using a custom-developed analysis tool. Reported variants were confirmed, if necessary, by an appropriate orthogonal method in the proband and, if submitted, in selected relatives. Additional sequencing technology and variant interpretation protocol has been previously described**. The general assertion criteria for variant classification are publicly available on the GeneDx ClinVar submission page (http://www.ncbi.nlm.nih.gov/clinvar/submitters/26957/)"

Aachen. For whole exome sequencing (WES), a DNA sample from the index patient was enriched using the Lotus™ DNA Library preparation kit (IDT, Coralville, Iowa) according to the manufacturers protocol. The exome library was sequenced on a NextSeq500 Sequencer with 2 × 75 cycles on a high-output flow cell (Illumina, San Diego, CA). FastQ-files were generated with bcl2fastq2 (Illumina). The alignment and variant calling was done using the SeqMule pipeline (v1.2.6). For variant detection, three different variant callers were used (GATKLite UnifiedGenotyper, SAMtools, FreeBayes consensus) and variants detected by at least two variant callers were taken for further assessment. Annotation and prioritization of variants were performed using KGGSeq (v1.0, 20/Jun./2018).

Synonymous variants and variants with a minor allele frequency (MAF) higher than 0.75% in public databases (i.e., gnomAD, EXAC, 1000 GP, ESP) were excluded.

Huston. Exome sequencing was performed as previously described in Yang et al.[2]

Supplemental references

1. Retterer, K., Juusola, J., Cho, M.T., Vitazka, P., Millan, F., Gibellini, F., Vertino-Bell, A., Smaoui, N., Neidich, J., Monaghan, K.G., et al. (2016). Clinical application of whole-exome sequencing across clinical indications. Genet Med *18*, 696–704.

2. Yang, Y., Muzny, D.M., Xia, F., Niu, Z., Person, R., Ding, Y., Ward, P., Braxton, A., Wang, M., Buhay, C., et al. (2014). Molecular findings among patients referred for clinical whole-exome sequencing. JAMA *312*, 1870–1879.